ADVANCED FUNCTIONAL MATERIALS
www.afm-journal.de

Materials Views
www.MaterialsViews.com

Atomically Defined Rare-Earth Scandate Crystal Surfaces

By *Josée E. Kleibeuker, Gertjan Koster,* Wolter Siemons, David Dubbink, Bouwe Kuiper, Jeroen L. Blok, Chan-Ho Yang, Jayakanth Ravichandran, Ramamoorthy Ramesh, Johan E. ten Elshof, Dave H. A. Blank,* and *Guus Rijnders*

The fabrication of well-defined, atomically sharp substrate surfaces over a wide range of lattice parameters is reported, which is crucial for atomically regulated epitaxial growth of complex oxide heterostructures. By applying a framework for controlled selective wet etching of complex oxides on the stable rare-earth scandates ($REScO_3$), $a_{pseudocubic} = 0.394 - 0.404$ nm, the large chemical sensitivity of $REScO_3$ to basic solutions is exploited, which results in reproducible, single-terminated surfaces. Time-of-flight mass-spectroscopy measurements show that after wet etching the surfaces are predominantly ScO_2 -terminated. Moreover, the morphology study of $SrRuO_3$ thin-film growth gives no evidence for mixed termination. Therefore, it is concluded that the $REScO_3$ surfaces are completely ScO_2 -terminated.

1. Introduction

Perovskite-type oxides, ABO_3, are an interesting class of materials as they exhibit diverse properties such as superconductivity, magnetism, and ferroelectricity.[1–3] Their oxygen backbone structure allows the formation of strained heteroepitaxial structures of high complexity, which result in advanced materials with enhanced functionality.[4–8] The conducting interfaces between $SrTiO_3$ and $LaAlO_3$, both wide-bandgap insulators, is an example of functionality determined at an atomic level.[5] Therefore it is essential to start with well-defined, crystalline substrates with single-terminated atomic planes, i.e., within the size of the unit cell.[9,10] However, in order to make major steps in the future, two important aspects that limit progress in the field of oxide electronics must be addressed: 1) Established techniques to obtain single termination are currently limited to one material, $SrTiO_3$, 2) proof of complete single termination has been difficult.

The (pseudo)cubic unit cell in the [001] is represented by a simplified stack of alternating layers of AO and BO_2 (**Figure 1a**). After creating a surface by, for instance, cleaving a single crystal, both layers are expected at the surface in equal proportion, which results in mixed terminated surfaces with steps of half or one unit cell high (0.2 and 0.4 nm, respectively; Figure 1b). However, single termination, with only 0.4 nm high steps (Figure 1c), is desirable for controlled growth at an atomic level. Therefore, it is crucial to treat the surface before growing complex oxide heterostructures. The typical surface treatment of perovskite-type oxides is high-temperature annealing which results in ordered, well-defined, crystalline surfaces. However, this treatment is inadequate for obtaining single termination and half-unit cell steps are still present. Kawasaki et al. introduced wet etching of $SrTiO_3$ (001), which was the first serious step towards single-terminated perovskite-type surfaces.[9] By etching the surface with an acidic NH_4F-buffered HF solution (BHF), they obtained a TiO_2-terminated surface, as confirmed by ion-scattering spectroscopy. To obtain single termination, the pH of the etchant is claimed to be crucial to achieve selectivity. However, since the treatment seriously depends on the $SrTiO_3$ surface quality prior to etching, this method often leads to uncontrolled wet etching. To etch $SrTiO_3$ in a controlled manner, Koster et al. introduced the formation of an intermediate Sr hydroxide complex at the topmost surface by immersion in water.[10] By subsequent short BHF etching, reproducible TiO_2-terminated surfaces were obtained. This method has been expanded to $SrTiO_3$ (111) by removing SrO_3^{4-}, to give a Ti-terminated surface.[11] However, the success of this technique to create single-terminated surfaces is limited to $SrTiO_3$ and is not suitable for other perovskite-type oxides. Note that recently Ngai et al. obtained predominant A-site-terminated $La_{0.18}Sr_{0.82}Al_{0.59}Ta_{0.41}O_3$ (LSAT) surfaces, with $a = 0.387$ nm, by tuning the vapor pressure of La near the LSAT surface during annealing.[12] This is an important step towards controlling the surface termination of LSAT. However, complete single-terminated LSAT remains difficult to achieve.

[*] J. E. Kleibeuker, Dr. G. Koster, D. Dubbink, B. Kuiper, J. L. Blok, Dr. J. E. ten Elshof, Prof. D. H. A. Blank, Prof. G. Rijnders
Faculty of Science and Technology and MESA+ Institute for Nanotechnology
University of Twente
7500 AE, Enschede, The Netherlands
E-mail: g.koster@utwente.nl
Dr. W. Siemons, Prof. C.-H. Yang, Prof. R. Ramesh
Department of Physics
University of California
Berkeley, CA 94720, USA
Prof. C.-H. Yang
Department of Physics and Institute for the NanoCentury
KAIST, Daejeon, 305–701, Republic of Korea
J. Ravichandran
Applied Science and Technology Graduate Group
University of California
Berkeley, CA 94720, USA

DOI: 10.1002/adfm.201000889

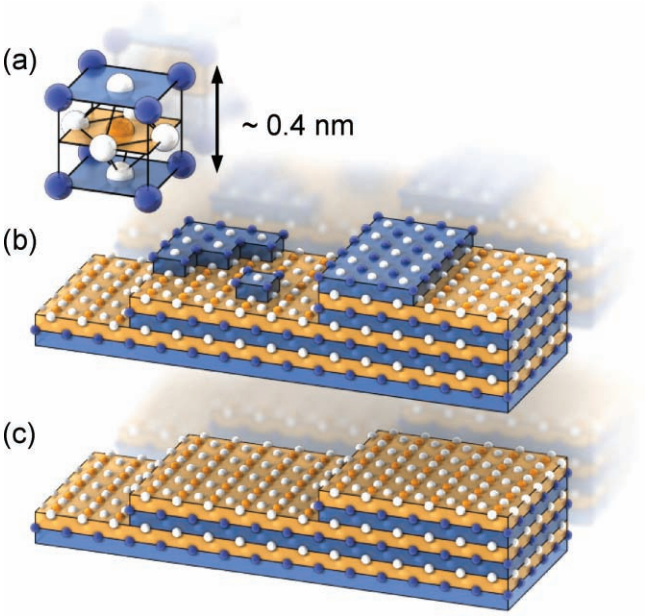

Figure 1. a) The ABO_3 unit cell, where A is typically a rare earth, alkaline earth or alkali metal ion, and B is often a transition metal ion. b) A schematic representation of a mixed-terminated surface with steps of 0.2, 0.4, and 0.6 nm high. c) A single-terminated BO_2 surface with steps of 0.4 nm high. The blue blocks correspond to the AO layer and the orange blocks to the BO_2 layer, with blue, orange, and white circles corresponding to A, B, and O ions, respectively.

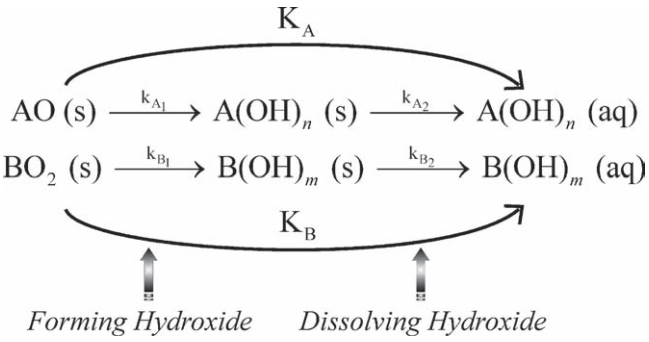

Scheme 1. Framework for controlled selective wet etching of perovskite-type oxides, where k_{A1}, k_{A2}, k_{B1}, and k_{B2} are the etching rate constants of the separate steps, and k_A and k_B are the overall etching rate constants of the AO and BO_2 layer, respectively. *n* and *m* depend on the valence of the cation.

To study the effects of strain on the physical behavior of complex heterostructures, it is essential that controllable single termination can be achieved on many perovskite-type oxide surfaces with a wide range of lattice parameters. Therefore, in this study, we introduce a framework for controlled selective wet etching of perovskite-type oxides and apply it to the rare-earth scandates ($REScO_3$). By using the large selectivity of basic solutions towards $REScO_3$, we accomplished the production of ScO_2-terminated surfaces, as measured by time-of-flight mass spectroscopy (TOF-MS). Despite the capability of chemical-probe techniques like TOF-MS to establish the dominant termination, these techniques are not capable of definitively proving complete single termination of perovskite-type surfaces. To overcome this difficulty, we combined TOF-MS with the enormous sensitivity of $SrRuO_3$ nucleation for the atomic composition of the surface to prove complete single termination.

2. Theoretical Basis

To develop a selective wet-etching framework for perovskite-type oxides, we considered wet etching as a combination of two steps: 1) forming a hydroxide, and 2) dissolving the hydroxide (**Scheme 1**). Moreover, we viewed perovskite-type oxides as a combination of two simple oxides: AO and BO_2. To establish single termination, selectivity has to be achieved by controlling both etching steps, for AO as well as for BO_2, through the right choice of the right etching solution(s), temperature, and duration. When the difference in overall etching rates of AO, k_A, and BO_2, k_B, is significant, both steps can be performed simultaneously. Another possible approach is to separate the steps in time, by exploiting the differences between the two etching processes. The latter approach was introduced by Koster et al. for $SrTiO_3$ (001).[10] The creation of single-terminated surfaces on other perovskite-type oxides can be achieved by controlling the rates of the two etching steps. High quality perovskite-type scandates are frequently used to create strained heterostructures, as they have a relatively large lattice parameter (0.394 – 0.404 nm) and can be grown without twinning.[13–16] However, surface treatments for perovskite-type scandates have hardly been addressed in the literature.[17,18] Therefore, it is a major challenge to develop controlled selective wet-etching treatments for perovskite-type scandates. Herein, we have used $DyScO_3$ as a model-system.

We first consider the chemistry of the stable sesquioxides of dysprosium and scandium, Dy_2O_3 and Sc_2O_3. As both sesquioxides are readily soluble in acidic solutions, selectivity for one of the atomic layers in $DyScO_3$ is expected to be minimal; this has been confirmed experimentally.[19] In basic solutions, like NaOH–deionized water (DI water), both sesquioxides are insoluble.[20] Therefore, small modifications, e.g., in the crystal structure, may be sufficient to induce some solubility of Sc and/or Dy in a basic etchant. Furthermore, selectivity could be induced through the difference in electrostatic bond strength (e.b.s.) of Sc and Dy.[21] In the sesquioxide structure, Dy and Sc have an e.b.s. of ½. However, in the perovskite structure, Dy and Sc have different coordination numbers and as a result the e.b.s. of Dy is ¼ while the e.b.s. of Sc is ½. This difference could point to an increased reactivity of Dy versus Sc. Therefore, we expect that the following reaction dominates the etching process:

$$Dy_2O_3(s) + 3H_2O(l) \xrightarrow{6OH^-(aq)} 2Dy(OH)_3(aq), \quad (1)$$

where OH^- acts as a catalyst. This should result in ScO_2-terminated surfaces. Moreover, as the lanthanoids behave chemically similar this methodology can be extrapolated to other $REScO_3$.

3. Results and Discussion

3.1. Wet Etching

We have used atomic force microscopy (AFM) to study the effects of the various steps of the surface treatment (**Figure 2**) on orthorhombic $DyScO_3$ (110), which corresponds to the pseudocubic $DyScO_3$ (001), where $a_{pseudocubic}$ (a_{pc}) = 0.3944 nm. As-received $DyScO_3$ substrates have a mixed-terminated surface that shows disordered step edges and islands on terraces with typical height differences of 0.2 and 0.4 nm (inset of Figure 2a). High-temperature annealing at 1000°C resulted in recrystallization of the surface, which led to regularly spaced steps with a height of 0.4 nm (Figure 2 a) that appears to be single termination. However, this is not a sufficient observation to conclude the existence of a complete single-terminated surface, as will be demonstrated below.

To obtain single-terminated $DyScO_3$ (110) surfaces in a controlled fashion, we applied controlled selective wet etching using 12 M NaOH–DI water solution. An annealed $DyScO_3$ substrate with a clear mixed-terminated surface was etched for different lengths of time to examine the required etching duration (Figure 2b and its corresponding line profile, Figure 2c). Figures 2d and e show the results after 20 min and 1 h of immersion in 12 M NaOH-DI water, respectively. After 20 min, the top layer is partly removed, as schematically depicted in Figure 2d. For this sample, after 1 h only steps of one unit cell high (0.4 nm) were observed (Figure 2f), which indicates single termination. Further exposure to 12 M NaOH–DI water appeared not to damage the surface since no etch pits were observed. The $DyScO_3$ surface remained stable after etching.

In addition to obtaining single termination, the treatment has to result in ordered, well-defined surfaces. Therefore, it is common to anneal the surface after etching, as in the case of $SrTiO_3$, to allow recrystallization which results in flat surfaces with straight steps.[9,10] However, our order of treatment is the opposite, namely first annealing and then etching. This order is important; when annealing at 1000 °C is performed after wet etching, mixed termination at the $DyScO_3$ surface recurs due to major bulk diffusion. Note that the temperature during thin-film growth is typically below the temperature at which major bulk diffusion occurs and therefore should not result in unintended mixed termination of the surface. As only one of the atomic layers is removed by 12 M NaOH–DI water (illustrated in Figure 2), the overall vicinal morphology is preserved after etching. The minimum duration of high-temperature annealing depends on the miscut. For substrates with a miscut of ≥0.1°, 4 h annealing at 1000 °C resulted in well-defined, ordered steps after etching. $DyScO_3$ (110) with a lower miscut requires a longer annealing time.[21]

3.2. Time-of-Flight Mass Spectroscopy

Having established single-terminated $DyScO_3$, we have to check which atomic layer, DyO or ScO_2, forms the topmost layer. Therefore, angle-dependent TOF-MS measurements (**Figure 3a**) were performed on three differently treated $DyScO_3$ surfaces: as-received, annealed, and wet-etched (Figure 3b).[22]

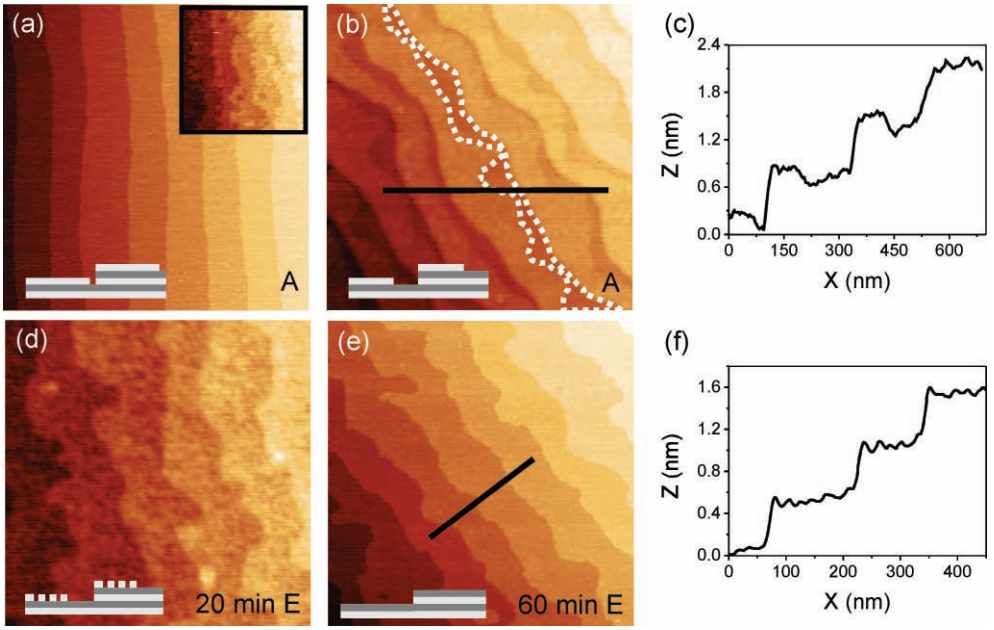

Figure 2. a) AFM height images of $DyScO_3$ (110) substrate after 4 h annealing at 1000°C with steps of one unit cell high. AFM height images of $DyScO_3$ after annealing b) after 30 min annealing at 1000 °C with clear mixed termination and steps of 0.2, 0.4, and 0.6 nm high, marked by the dashed line and also shown in its corresponding line profile (c); subsequently after d) 20 min immersion in 12 M NaOH-DI water and after e) 1 h immersion in 12 M NaOH–DI water with its corresponding line profile showing only 0.4 nm steps (f). The labels A and E denote substrates after annealing and after wet etching, respectively. The inset of (a) shows an AFM height image of an as-received $DyScO_3$ (110) substrate. The sketches give a schematic representation of the surface layer. All AFM images represent 1 × 1 μm².

Full-range mass spectra of the three samples were collected at different azimuthal angles and normalized with respect to the integrated intensity of the Sc peak. Figure 3b shows the Sc/Dy intensity ratio as function of the azimuthal angle for the three different samples. No clear maxima were observed in the spectra of the as-received and annealed $DyScO_3$ surfaces, which indicates mixed termination. On the other hand, the wet-etched sample shows clear maxima at 45° and 135°. This observation is due to blocking of Dy by the topmost Sc atoms and can only be observed when the surface is predominantly ScO_2-terminated (Figure 3c). As $Sc(OH)_6^{3-}$ is also soluble in basic solutions, it is most likely that the difference in the rate of forming a hydroxide, $k_{Dy1} >> k_{Sc1}$, is crucial for achieving selectivity towards ScO_2-terminated $DyScO_3$ (110). This explains why the NaOH–DI water solution does not etch beyond the top layer and no etch pits are created.

As the chemical behavior of all lanthanoids is similar and the etching rate of the ScO_2 layer is minimal, we have applied the wet-etching treatment to other $REScO_3$, like $GdScO_3$ (a_{pc} = 0.397 nm) and $NdScO_3$ (a_{pc} = 0.401 nm). TOF-MS analysis on these substrates (Figure 3d and e) shows clear maxima for the wet etched surfaces at 45° and 135°, which indicates Sc-terminated surfaces. This result implies that the surface treatment is effective for all $REScO_3$.

Note that it is likely that oxygen vacancies, structural reconstruction, and/or adsorbents occur at the surface, as ScO_2 is polar, but this should not affect the predominant type of cation at the top-most layer.

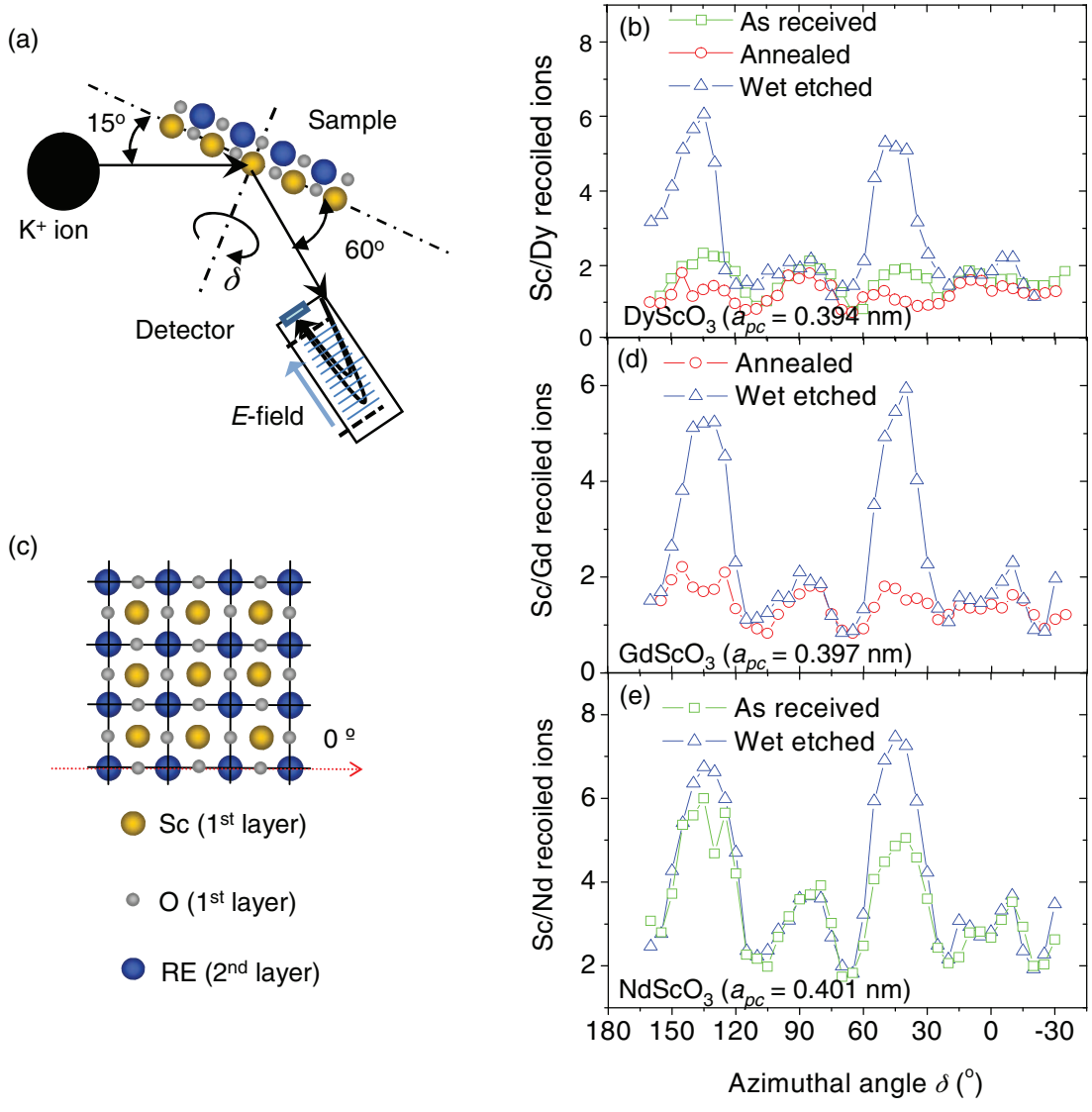

Figure 3. a) Schematic picture of the TOF-MS setup, where δ denotes the azimuthal angle. The yellow, blue, and gray circles correspond to Sc, RE, and O ions, respectively. b) Azimuthal maps of three differently treated $DyScO_3$ (110) surfaces are shown: as received, 4-h annealed and 4-h annealed and 1-h wet etched. Maximum blocking of Dy was observed on the wet-etched surface at 45° and 135°. c) A top-down view of the atomic arrangement on an unreconstructed ScO_2-terminated $REScO_3$ (110) surface, where the arrow indicates the direction of 0° azimuthal angle. d) Azimuthal maps of a 4-h annealed and a 4-h annealed and 1-h wet etched $GdScO_3$ (110) with maximum blocking of Gd at 45° and 135° after wet etching. e) Azimuthal maps of an as-received and a 4-h annealed and 1-h wet-etched $NdScO_3$ (110) with maximum blocking of Nd at 45° and 135°.

3.3. $SrRuO_3$ Growth

Despite the suitability of TOF-MS and other chemical probing techniques to determine the dominant terminating layer, their ability to prove complete single termination is compromised since the elements present at the surface are also present in the bulk. Therefore, we introduce a simple method to determine complete single termination of $DyScO_3$: growth of $SrRuO_3$. As the nucleation of $SrRuO_3$ is very sensitive to differences in surface diffusivity (see Experimental Section for specific growth conditions), the presence of small areas of mixed termination is amplified, as can easily be observed by AFM and/or scanning tunneling microscopy (STM) in the morphology of the $SrRuO_3$ layer.[23–25] From $SrRuO_3$ on $SrTiO_3$ (001) studies, it is known that two-dimensional $SrRuO_3$ growth occurs when the substrate is single-terminated (an example is given in **Figure 4a** with its corresponding line profile in Figure 4b).[23] However, deep trenches in grown $SrRuO_3$ films are typically observed when the $SrTiO_3$ surface is even slightly mixed-terminated (Figure 4c).[24,25] On $DyScO_3$, we observed the same phenomena. Figure 4d shows a flat film of $SrRuO_3$ with terraces of one unit cell high and without deep trenches, on an annealed and subsequently wet-etched $DyScO_3$ substrate (see Figure 4e for its corresponding line profile). This indicates 100% single termination of $DyScO_3$ after wet etching. Note that based on the lateral resolution being better than 10 nm and the fact that we do not observe domains with step heights different from 0.4 nm on a micron-size scan size, we conclude that we have complete single termination with a better than 1% uncertainty. On annealed $DyScO_3$, random line growth was observed (Figure 4f), which indicates mixed-terminated $DyScO_3$ surface after annealing. These results are in agreement with the TOF-MS measurements and confirm complete single termination after wet etching.

To verify the quality of the growth of $SrRuO_3$ on $SrTiO_3$ and on $DyScO_3$, the film structure and surface morphology were monitored by reflective high energy electron diffraction (RHEED; **Figure 5**). The intensity versus time of the specular spot (00) of the two-dimensional grown $SrRuO_3$ films on $SrTiO_3$, and on $DyScO_3$; both showed one clear oscillation (Figure 5a and b, respectively). After this oscillation, step-flow-like growth (one unit cell high island nucleation, but constant overall morphology and constant RHEED intensity) occurred, which results in meandering step edges (Figure 4a and d).[23,26,27] The RHEED patterns before and after $SrRuO_3$ growth (Figure 5c–f) confirmed the crystallinity of the surface layer.

4. Conclusions

In conclusion, we have developed a reliable method to obtain complete ScO_2-terminated $RESCO_3$ by following our framework for controlled selective wet etching of perovskite-type oxides. We made use of the large difference in etching rates of REO and ScO_2 in a basic solution. Our wet-etching framework can be applied to other perovskite-type oxides. In the case of perovskite-type aluminates, e.g., $LaAlO_3$ and $YAlO_3$, the high solubility of Al in acidic as well as in basic solutions can be utilized, resulting in A-site terminated surfaces. Finally, we showed that

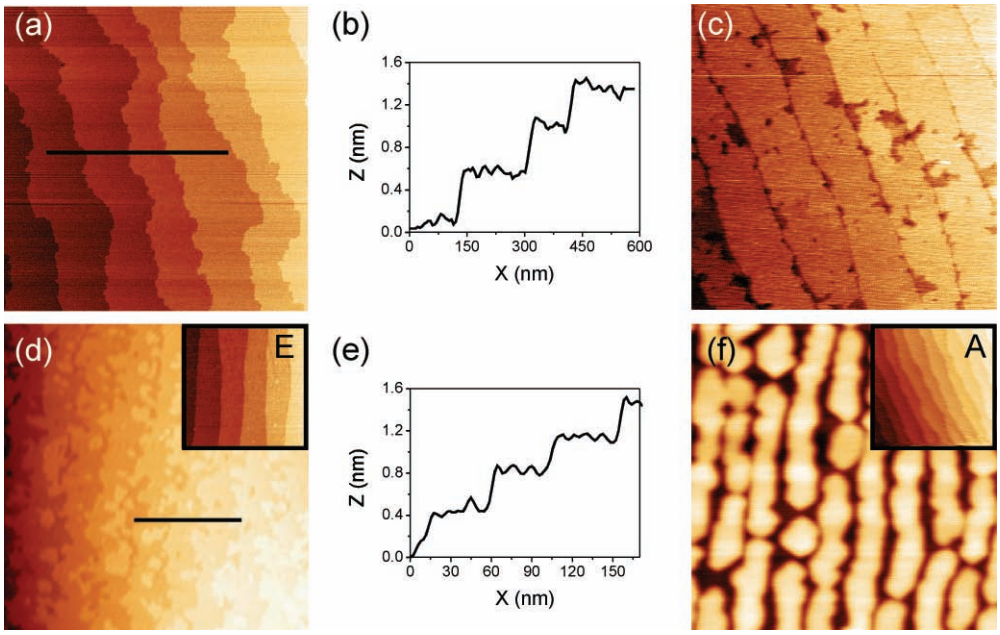

Figure 4. In situ STM height images of a) 2 nm $SrRuO_3$ film on TiO_2-terminated $SrTiO_3$ (001) showing steps of one unit cell height with its corresponding height profile (b) and of c) 3 nm $SrRuO_3$ on mixed-terminated $SrTiO_3$ (001) with trenches approximately 3 nm deep. d) In situ STM height image of 8 nm film of $SrRuO_3$ on annealed and subsequently 1-h wet-etched $DyScO_3$ (110) showing steps one unit cell high with its corresponding height profile (e). f) AFM height image of 4 to 8 nm high lines of $SrRuO_3$ on annealed $DyScO_3$ (110). The insets show AFM height images of the corresponding substrates, where E and A denote substrates after wet etching and after annealing, respectively. Images (a), (c) and (d) and both insets represent $1 \times 1\ \mu m^2$, image (f) represents $500 \times 500\ nm^2$.

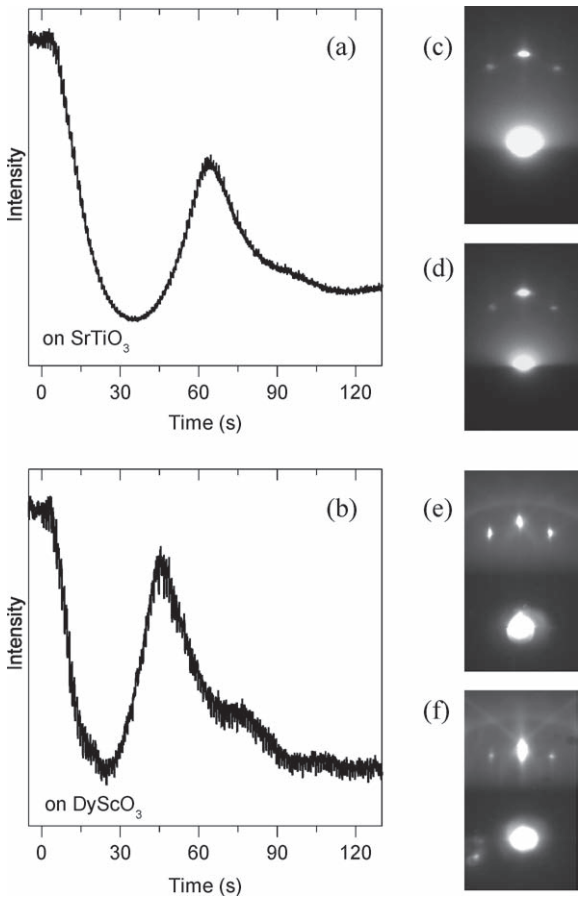

Figure 5. In situ RHEED analysis of $SrRuO_3$ growth. The intensity versus time of the specular spot during the initial $SrRuO_3$ growth on $SrTiO_3$ (a) and on $DyScO_3$ (b). The RHEED patterns before and after growth on $SrTiO_3$ (c and d, respectively) and on $DyScO_3$ (e and f, respectively) show the crystalline quality of the surfaces.

the combination of TOF-MS analysis and $SrRuO_3$ nucleation and growth is a powerful method to determine the termination of perovskite-type surfaces and to verify their complete single termination. This result enables studies on new, atomically controlled, heteroepitaxial systems.

5. Experimental Section

Surface Treatment: $DyScO_3$ (110) substrates (CrysTec GmbH, Germany) of $5 \times 5 \times 0.5$ mm^3 were annealed at 1000°C for 30 min to 12 h with a 150 mL min^{-1} O_2 flow. After cleaning with ethanol, the annealed substrates were successively immersed in 12 M NaOH–DI water solution (etching) and in 1 M NaOH–DI water solution (preventing precipitation). Both immersion steps were carried out in an ultrasonic bath for 10 min to 1 h. Finally, the samples were rinsed with DI water (three times) and ethanol.

$NdScO_3$ (110) and $GdScO_3$ (110) (CrysTec GmbH, Germany) of $5 \times 5 \times 0.5$ mm^3 were annealed at 1000 °C for 4 h under flowing O_2. The annealed substrates were successively immersed for 1 h in 12 M NaOH–DI water solution (etching) and 30 min in 1 M NaOH–DI water solution (preventing precipitation). Both immersion steps were carried out in an ultrasonic bath. Finally, the samples were rinsed with DI water (three times) and ethanol.

$SrTiO_3$ (001) substrates (CrysTec GmbH, Germany) of $5 \times 5 \times 0.5$ mm^3 were treated according to the method described by Koster et al. and Ohnishi et al.[10,28]

$SrRuO_3$ Growth: $SrRuO_3$ was grown using pulsed laser deposition (PLD) at a pressure of 0.3 mbar, 50%/50% O_2/Ar. The substrate temperature was approximately 600–640 °C. $SrRuO_3$ was deposited with a repetition rate of 1 Hz and a fluence of 2.1 J cm^{-2}, using a KrF laser (λ = 248 nm). $SrRuO_3$ growth was studied in situ using RHEED. Note that the sensitivity to selective nucleation depends on the growth conditions.

Surface Analysis: The surface morphology was characterized ex situ using tapping mode AFM (Veeco's Dimension Icon, United Kingdom). STM was performed in situ on a variable-temperature scanning probe microscope (VT-SPM; Omicron NanoTechnology GmbH, Germany). Before the TOF-MS measurements, the substrates were cleaned in trichloroethene, acetone, and isopropanol in turn. All cleaning steps were carried out in an ultrasonic bath. After installing the substrates inside the ultrahigh-vacuum TOF-MS chamber, the samples were heated to 500–600 °C with 0.13 mbar O_2 to remove hydrocarbons on the substrates. TOF-MS measurements (Ionwerks' time-of-flight mass spectrometer, USA) were performed using potassium ions accelerated to 10 keV. The incoming angle, α, was fixed at 15°, while the azimuthal angle, δ, was varied. Ion collection was done in shadowing mode, i.e. ions were collected at 60°, an angle much larger than the incident angle. Ions with masses up to 200 amu were detected. The measurements were performed at room temperature.

Acknowledgements

This work is financially supported by the Netherlands Organisation for Scientific Research (NWO) through a VIDI grant to G.R. and a Rubicon grant to W.S.

Received: May 4, 2010
Revised: June 17, 2010
Published online: August 23, 2010

[1] J. G. Bednorz, K. A. Müller, *Z. Phys. B* **1986**, *64*, 189.
[2] J.-H. Park, E. Vescovo, H.–J. Kim, C. Kwon, R. Ramesh, T. Venkatesan, *Nature* **1998**, *392*, 794.
[3] W. J. Merz, *Phys. Rev.* **1949**, *76*, 1221.
[4] G. Rijnders, D. H. A. Blank, *Nature* **2005**, *433*, 369.
[5] A. Ohtomo, H. Y. Hwang, *Nature* **2004**, *427*, 423.
[6] H. N. Lee, H. M. Christen, M. F. Chisholm, C. M. Rouleau, D. H. Lowndes, *Nature* **2005**, *433*, 395.
[7] K. Ueda, H. Tabata, T. Kawai, *Science* **1998**, *280*, 1064.
[8] D. P. Norton, B. C. Chakoumakos, J. D. Budai, D. H. Lowndes, B. C. Sales, J. R. Thompson, D. K. Christen, *Science* **1994**, *265*, 2074.
[9] M. Kawasaki, K. Takahashi, T. Maeda, R. Tsuchiya, M. Shinohara, O. Ishiyama, T. Yonezawa, M. Yoshimoto, H. Koinuma, *Science* **1994**, *266*, 1540.
[10] G. Koster, B. L. Kropman, G. J. H. M. Rijnders, D. H. A. Blank, H. Rogalla, *Appl. Phys. Lett.* **1998**, *73*, 2920.
[11] J. Chang, Y.-S. Park, S.-K. Kim, *Appl. Phys. Lett.* **2008**, *92*, 152910.
[12] J. H. Ngai, T. C. Schwendemann, A. E. Walker, Y. Segal, F. J. Walker, E. I. Altman, C. H. Ahn, *Adv. Mater.* **2010**, *22*, 2945
[13] K. J. Choi, M. Biegalski, Y. L. Li, A. Sharan, J. Schubert, R. Uecker, P. Reiche, Y. B. Chen, X. Q. Pan, V. Gopalan, L.-Q. Chen, D. G. Schlom, C. B. Eom, *Science* **2004**, *306*, 1005.
[14] J. H. Haeni, P. Irvin, W. Chang, R. Uecker, P. Reiche, Y. L. Li, S. Choudhury, W. Tian, M. E. Hawley, B. Craigo, A. K. Tagantsev,

X. Q. Pan, S. K. Streiffer, L. Q. Chen, S. W. Kirchoefer, J. Levy, D. G. Schlom, *Nature* **2004**, *430*, 758.
[15] C. Adamo, X. Ke, H. Q. Wang, H. L. Xin, T. Heeg, M. E. Hawley, W. Zander, J. Schubert, P. Schiffer, D. A. Muller, L. Maritato, D. G. Schlom, *Appl. Phys. Lett.* **2009**, *95*, 112504.
[16] R. Uecker, B. Velickov, D. Klimm, R. Bertram, M. Bernhagen, M. Rabe, M. Albrecht, R. Fornari, D. G. Schlom, *J. Cryst. Growth* **2008**, *310*, 2649.
[17] S. Karimoto, M. Naito, *Appl. Phys. Lett.* **2004**, *84*, 2136.
[18] S. Venkatesan, B. J. Kooi, J. T. M. De Hosson, A. H. G. Vlooswijk, B. Noheda, *J. Appl. Phys.* **2007**, *102*, 104105.
[19] D. R. Lide, in *CRC Handbook of Chemistry and Physics*, CRC Press/Taylor and Francis, Boca Raton, FL **2008**.
[20] L. Pauling, in *The Nature of the Chemical Bond*, Cornell University Press, Ithaca, NY **1960**.
[21] Note that longer annealing may influence the minimum required etching time.
[22] J. Wayne Rabalais, in *Principles and Applications of Ion Scattering Spectrometry*, John Wiley & Sons, Inc., Hoboken, NJ **2003**.
[23] G. Rijnders, D. H. A. Blank, J. Choi, C. B. Eom, *Appl. Phys. Lett.* **2004**, *84*, 505.
[24] R. Bachelet, F. Sanchez, J. Santiso, C. Munuera, C. Ocal, J. Fontcuberta, *Chem. Mater.* **2009**, *21*, 2494.
[25] W. Siemons, *Ph.D. Thesis*, University of Twente, The Netherlands **2008**.
[26] J. Choi, C. B. Eom, G. Rijnders, H. Rogalla, D. H. A. Blank, *Appl. Phys. Lett.* **2001**, *79*, 1447.
[27] W. Hong, H. N. Lee, M. Yoon, H. M. Christen, D. H. Lowndes, Z. Suo, Z. Zhang, *Phys. Rev. Lett.* **2005**, *95*, 095501.
[28] T. Ohnishi, K. Shibuya, M. Lippmaa, D. Kobayashi, H. Kumigashira, M. Oshima, H. Koinuma, *Appl. Phys. Lett.* **2004**, *85*, 272.